Inorganic Chemistry

Article

Synthesis and Structure of [2 × 2] Molecular Grid Copper(II) and Nickel(II) Complexes with a New Polydentate Oxime-Containing Schiff Base Ligand

Yurii S. Moroz,[†] Kinga Kulon,[‡] Matti Haukka,[§] Elżbieta Gumienna-Kontecka,[‡] Henryk Kozłowski,*[‡] Franc Meyer,*[‖] and Igor O. Fritsky*[†]

Department of Chemistry, Kiev National Taras Shevchenko University, 01601 Kiev, Ukraine, Faculty of Chemistry, University of Wroclaw, F. Joliot-Curie 14, 50-383 Wroclaw, Poland, Department of Chemistry, University of Joensuu, P.O. Box 111, 80101 Joensuu, Finland, and Institut für Anorganische Chemie, Georg-August-Universität Göttingen, Tammannstrasse 4, D-37077 Göttingen, Germany

A new polynucleating oxime-containing Schiff base ligand, 2-hydroxyimino-*N′*-[1-(2-pyridyl)ethylidene]propanohydrazone (H**pop**), has been synthesized and fully characterized. pH potentiometric, electrospray ionization mass spectrometric, and spectrophotometric studies of complex formation in H_2O/DMSO solution confirmed the preference for polynuclear complexes with 3d metal ions. Single-crystal X-ray diffraction analyses of $[Ni_4(\textbf{pop})_4(HCOO)_4] \cdot 7H_2O$ (**1**), $[Cu_4(\textbf{pop}\text{-}H)_4(HCOOH)_4] \cdot H_2O$ (**2**), and $[Cu_4(\textbf{pop}\text{-}H)_4(H_2O)_4] \cdot 9H_2O$ (**3**) indicated the presence of a [2 × 2] molecular grid structure in all three compounds but distinct configurations of the cores: a head-to-tail ligand arrangement with overall S_4 symmetry of the grid in the Cu^{2+} complexes as opposed to a head-to-head ligand arrangement with (noncrystallographic) C_2 grid symmetry for the Ni^{2+} complex. A cryomagnetic study of **3** revealed intramolecular ferromagnetic exchange between copper ions in the grid, while in **1**, antiferromagnetic interactions between the metal ions were observed.

Introduction

In the past few decades, self-assembled polymetallic grid structures have attracted considerable attention, mainly because of their potentially useful electronic, magnetic, and photophysical properties, which are being discussed in the context of molecule-based information storage devices.[1,2] On a more fundamental level, grid-shaped complexes have allowed chemists to address basic questions concerning metal-assisted self-assembly, which has evolved as a powerful and versatile synthetic methodology for the construction of supramolecular aggregates.[3,4] It is obvious that the design of gridlike metal ion arrays relies on directing coordination algorithms comprising the preferred coordination geometry of the metal ion and the binding sites of the ligand.[5] Unique features may result from additional functional sites in the periphery of the ligand that can be used for protonic modulation or further decoration of the grid.[6,7] It was recently reported that dicarboxamide derivatives of pyrazine provide an effective tool for controlling the nuclearity of metal complexes by means of base-dependent equilibria between deprotonated and zwitterionic forms of the ligands.[8,9]

* To whom correspondence should be addressed. E-mail: henrykoz@wchuwr.pl (H.K.), franc.meyer@chemie.uni-goettingen.de (F.M.), ifritsky@yahoo.com (I.O.F.).

[†] Kiev National Taras Shevchenko University.
[‡] University of Wroclaw.
[§] University of Joensuu.
[‖] Georg-August-Universität Göttingen.

(1) Ruben, M.; Rojo, J.; Romero-Salguero, F. J.; Uppadiene, L. H.; Lehn, J.-M. *Angew. Chem., Int. Ed.* **2004**, *35*, 3644–3662.
(2) Ruben, M.; Lehn, J.-M.; Müller, P. *Chem. Soc. Rev.* **2006**, *35*, 1056–1067.
(3) Lehn, J.-M. *Science* **2002**, *295*, 2400–2403.
(4) Nitschke, J. R.; Lehn, J.-M. *Proc. Natl. Acad. Sci. U.S.A.* **2003**, *100*, 11970–11974.
(5) (a) Lan, Y.; Kennepohl, D. K.; Moubaraki, B.; Murray, K. S.; Cashion, J. D.; Jameson, G. B.; Brooker, S. *Chem.—Eur. J.* **2003**, *9*, 3772–3784. (b) Petitjean, A.; Kyritsakas, N.; Lehn, J.-M. *Chem. Commun.* **2004**, 1168–1169. (c) Price, J. R.; Lan, Y.; Jameson, G. B.; Brooker, S. *Dalton Trans.* **2006**, 1491–1494.
(6) Ruben, M.; Lehn, J.-M.; Vaughan, G. *Chem. Commun.* **2003**, 1338–1339.
(7) Klingele, J.; Prikhod'ko, A. I.; Leibeling, G.; Demeshko, S.; Dechert, S.; Meyer, F. *Dalton Trans.* **2007**, 2003–2013.

Among the variety of grid-type systems, the [2 × 2] molecular grids are most abundant.[10] They have been obtained for various ligand systems with almost all of the 3d metal ions. Oligotopic hydrazone ligands, often heterotopic ones, have become increasingly popular in the field and have enabled the construction of grids having dimensions as large as [5 × 5]. Among their advantages is the ease of their formation via straightforward Schiff base condensations.[11–13]

In previously reported Ni(II), Mn(II), and Co(II) [2 × 2] molecular grids having the metal ions connected through amide oxygen atoms or a hydrazone group, antiferromagnetic coupling between the metal ions is usually prevalent.[9,14,15] On the other hand, for Cu(II) [2 × 2] molecular grids with the same linkers between the metal ions, significant ferromagnetic coupling has been observed.[12,16,17] For other Cu(II) molecular grids, having substituted pyrazoles as bridging units, the presence of predominantly antiferromagnetic coupling between the metal ions was found to be dependent on peculiarities of the molecular structure.[7,18–20] In many of the reported cases, the coordination spheres of the metal ions were saturated by donor atoms from the compartmental ligands forming the grid-type array, and there was no possibility of further connecting the grids to produce higher supramolecular aggregates.

Here we report the synthesis and investigation of a new, well-designed polynucleating ligand, 2-hydroxyimino-N'-[1-(2-pyridyl)ethylidene]propanohydrazone (H**pop**), which exhibits a strong ability to form [2 × 2] Cu(II) and Ni(II) molecular grids that, as a result of the presence of labile

sites in their coordination spheres, may potentially be used as building blocks to obtain metal complexes of higher nuclearity.

Experimental Section

General Information. All of the reagents used in this work were of analytical grade and used without further purification. For solubility reasons, the physicochemical properties of the ligand and its nickel(II) and copper(II) complexes were examined in a 10/90 (v/v) dimethyl sulfoxide (DMSO)/water mixture. The ionic strength (I) was adjusted to 0.1 M using KNO_3. The experiments were carried out at 25 °C.

Physical Measurements. Potentiometric titrations of H**pop** and its complexes with Ni^{2+} and Cu^{2+} were performed using a MOLSPIN pH meter system with a total sample volume of 1.8 mL. The free hydrogen ion concentrations were measured using a Russel CMAW 711 semicombined electrode calibrated daily with respect to hydrogen ion concentration using HNO_3.[21] The calculated ionic product for the 10/90 (v/v) DMSO/water solution was 14.04. As a titrant, 0.1 M NaOH was added from a 0.250 mL micrometer syringe that was calibrated by weight titration and titration of standard materials. The exact concentration of the ligand was determined using the method of Gran.[22] The ligand concentration was $3 × 10^{-3}$ M, and the metal-to-ligand molar ratios were 1/2, 1/3, and 1/4 for Ni(II) and 1/1, 1/2, and 1/4 for Cu(II). The potentiometric data, which were collected over a pH range of 2–11, were refined with the SUPERQUAD program.[23] Standard deviations computed by SUPERQUAD refer to random errors only.

Absorption spectra were recorded using a Beckman DU 650 spectrophotometer. Electron paramagnetic resonance (EPR) spectra were recorded using a Bruker ESP 300E spectrometer at the X-band frequency (9.3 GHz) at 120 K. In the spectroscopic measurements, concentrations and metal-to-ligand molar ratios were similar to those used in the potentiometric titrations. The values of ϵ and the EPR parameters were calculated at the maximum concentrations of the respective species obtained from the potentiometric data.
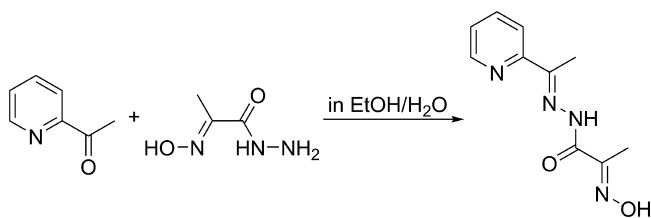
Variable-temperature magnetic susceptibility data (2–300 K) were acquired on a powdered sample using a Quantum Design MPMS-5 SQUID magnetometer. Corrections for the diamagnetism of the ligand were applied using Pascal's constants.

Electrospray ionization mass spectrometry (ESI-MS) data were collected using a Finigan TSQ 700 mass spectrometer. The complexes were dissolved in methanol, 1/2 (v/v) methanol/water, or 1/2 (v/v) methanol/DMSO solutions having concentrations of 10^{-4}–10^{-6} M. Interpretation of the mass spectra of mono- and polynuclear complexes and calculation of isotope distribution patterns for positive-ion clusters were performed with the help of the Isopro 3.0 program.

^{1}H NMR spectra (400 MHz) were recorded using a Bruker AC-400 spectrometer at 293 K. IR spectra (KBr pellets) were recorded using a Perkin-Elmer 180 spectrometer in the wavenumber range 200–4000 cm^{-1}. Elemental analysis was performed using a Perkin-Elmer 2400 CHN analyzer.

(8) (a) Hausmann, J.; Jameson, G. B.; Brooker, S. *Chem. Commun.* **2003**, 2992–2993. (b) Hausmann, J.; Boas, J. F.; Pilbrow, J. R.; Moubaraki, B.; Murray, K. S.; Berry, K. J.; Hunter, K. A.; Jameson, G. B.; Boyd, P. D. W.; Brooker, S. *Dalton Trans.* **2007**, 633–645.

(9) Cati, D. S.; Ribas, J.; Ribas-Arino, J.; Stoeckli-Evans, H. *Inorg. Chem.* **2004**, *43*, 1021–1030.

(10) Waldmann, O. *Coord. Chem. Rev.* **2005**, *249*, 2550–2566.

(11) (a) Dey, S. K.; Thompson, L. K.; Dawe, L. N. *Chem. Commun.* **2006**, 4967–4969. (b) Parsons, S. R.; Thompson, L. K.; Dey, S. K.; Wilson, C.; Howard, J. A. K. *Inorg. Chem.* **2006**, *45*, 8832–8834. (c) Dawe, L. N.; Abedin, T. S. M.; Kelly, T. L.; Thompson, L. K.; Miller, D. O.; Zhao, L.; Wilson, C.; Leech, M. A.; Howard, J. A. K. *J. Mater. Chem.* **2006**, *16*, 2645–2659. (d) Dawe, L. N.; Thompson, L. K. *Angew. Chem., Int. Ed.* **2007**, *46*, 7440–7444. (e) Dey, S. K.; Abedin, S. M.; Dawe, L. N.; Tandon, S. S.; Collins, J. L.; Thompson, L. K.; Postnikov, A. V.; Alam, M. S.; Müller, P. *Inorg. Chem.* **2007**, *46*, 7767–7781.

(12) Roy, S.; Mandal, T. N.; Barik, A. K.; Pal, S.; Butcher, R. J.; El Fallah, M. S.; Tercero, J.; Kumar, K. S. *Dalton Trans.* **2007**, 1229–1234.

(13) Barboiu, M.; Ruben, M.; Blasen, G.; Kyritsakas, N.; Chacko, E.; Dutta, M.; Radekovich, O.; Lenton, K.; Brook, D. J. R.; Lehn, J.-M. *Eur. J. Inorg. Chem.* **2006**, 784–792.

(14) Cheng, L.; Zhang, W.-X.; Ye, B.-H.; Lin, J.-B.; Chen, X.-M. *Inorg. Chem.* **2007**, *46*, 1135–1143.

(15) Manoj, E.; Prathapachandra Kurup, M. R.; Fun, H.-K.; Punnoose, A. *Polyhedron* **2007**, *26*, 4451–4462.

(16) Matthews, C. J.; Avery, K.; Xu, Z.; Thompson, L. K.; Zhao, L.; Miller, D. O.; Biradha, K.; Poirier, K.; Zaworotko, M. J.; Wilson, C.; Goeta, A. E.; Howard, J. A. K. *Inorg. Chem.* **1999**, *38*, 5266–5276.

(17) Xu, Z.; Thompson, L. K.; Miller, D. O. *J. Chem. Soc., Dalton Trans.* **2002**, 2462–2466.

(18) Zhang, H.; Fu, D.; Ji, F.; Wang, G.; Yu, K.; Yao, T. *J. Chem. Soc., Dalton Trans.* **1996**, 3799–3803.

(19) Mann, K. L. V.; Psillakis, E.; Jeffery, J. C.; Rees, L. H.; Harden, N. M.; McCleverty, J. A.; Ward, M. D.; Gatteschi, D.; Totti Mabbs, F.; Frank, E.; McInnes, E. J. L.; Riedi, P. C.; Smith, G. M. *J. Chem. Soc., Dalton Trans.* **1999**, 339–348.

(20) van der Vlugt, J. I.; Demeshko, S.; Dechert, S.; Meyer, F. *Inorg. Chem.* **2008**, *47*, 1576–1585.

(21) Irving, H. M.; Miles, M. G.; Pettit, L. D. *Anal. Chim. Acta* **1967**, *38*, 475–488.

(22) Gran, G. *Acta Chem. Scand.* **1950**, *29*, 559–577.

(23) Gans, P.; Sabatini, A.; Vacca, A. *J. Chem. Soc., Dalton Trans.* **1985**, 1195–1200.

(24) Fritsky, I. O.; Kozłowski, H.; Sadler, P. J.; Yefetova, O. P.; Światek-Kozłowska, J.; Kalibabchuk, V. A.; Glowiak, T. *J. Chem. Soc., Dalton Trans.* **1998**, 3269–3274.

Scheme 1. Synthesis of the Ligand 2-Hydroxyimino-N'-[1-(2-pyridyl)ethylidene]propanohydrazone (H**pop**)

Table 1. Crystal Data and Structure Refinement Parameters for Compounds **1**–**3**

	1	2	3
empirical formula	$C_{44}H_{66}N_{16}O_{23}Ni_4$	$C_{44}H_{52}N_{16}O_{18}Cu_4$	$C_{40}H_{66}N_{16}O_{21}Cu_4$
formula weight	1421.97	1347.16	1361.25
T (K)	120(2)	120(2)	120(2)
λ (Å)	0.71073	0.71073	0.71073
crystal system	monoclinic	tetragonal	monoclinic
space group	$P2_1/n$	$P4_2/n$	$P2/n$
a (Å)	11.6193(2)	15.4644(10)	12.7072(5)
b (Å)	34.4991(6)	15.4644(10)	11.1902(5)
c (Å)	15.8408(3)	11.4200(4)	21.2402(7)
α (deg)	90	90	90
β (deg)	108.252(1)	90	104.094(3)
γ (deg)	90	90	90
V (Å³)	6030.40(19)	2731.1(3)	2929.4(2)
Z	4	2	2
D_{calc} (g cm^{-3})	1.566	1.638	1.543
μ (cm^{-1})	13.19	16.23	15.17
R1	0.0681	0.0436	0.0573
wR2	0.1531	0.0919	0.1283

Synthesis, Purification, and Characterization of the Ligand 2-Hydroxyimino-N'-[1-(2-pyridyl)ethylidene]propanohydrazone (Hpop). 2-Acetylpyridine (1.2 mL, 0.0107 mol) was added to 20 mL of a stirred, warm ethanol/water solution of 2-(hydroxyimino)propanohydrazide[24] (1.17 g, 0.01 mol) (Scheme 1). After 6 h of stirring at 60 °C, the solution was cooled, and a white precipitate was formed immediately. The precipitate was filtered off, washed with water and acetone, and dried under vacuum. Yield: 1.59 g, 72%.

^{1}H NMR (400.13 MHz, DMSO-d_6, 25 °C): δ 12.12 (s, 1H, N–OH), 10.24 (s, 1H, NH), 8.61 (dt, 1H, Py-6, $J_{6,5}$ = 4.8 Hz, $J_{6,4}$ = 1.8 Hz), 8.07 (d, 1H, Py-3, $J_{3,4}$ = 7.8 Hz), 7.86 (td, 1H, Py-4, $J_{4,5,3}$ = 7.8 Hz, $J_{4,6}$ = 1.8 Hz), 7.42 (ddd, 1H, Py-5, $J_{5,6}$ = 4.8 Hz, $J_{5,4}$ = 7.8 Hz, $J_{5,3}$ = 1.2 Hz), 2.38 [s, 3H, CH$_3$(Py)], 1.99 (s, 3H, CH$_3$). IR (KBr) ν (cm^{-1}): 1660 (C=O$_{amid\ 1}$), 1030 (N–O$_{oxim}$), 3340 (N–H$_{as}$). Anal. Calcd for $C_{10}H_{12}N_4O_2$: C, 54.54; H, 5.49; N, 25.44. Found: C, 54.41; H, 5.62; N, 25.42.

Syntheses of Coordination Compounds. [Ni$_4$(pop)$_4$(HCOO)$_4$]·7H$_2$O (1). To 15 mL of a warm solution of H**pop** (0.022 g, 0.0001 mol) in methanol (15 mL) was added a solution of Ni(NO$_3$)$_2$·6H$_2$O (0.029 g, 0.0001 mol) and HCOOK (0.0084 g, 0.0001 mol) in water (10 mL) followed by 1 mL of 0.1 M KOH. The resulting dark-red mixture was stirred for 30 min and left in a test tube for crystallization in air. Brown needle crystals were formed after 25 days. Yield: 45%.

ESI-MS, m/z (%): 831.02 (60), {[Ni$_3$(**pop**-H)$_3$] + H}$^+$; 1106.91 (92), {[Ni$_4$(**pop**-H)$_4$] + H}$^+$; 554.00 (100), {[Ni$_4$(**pop**-H)$_4$] + 2H}$^{2+}$; 1152.96 (48), {[Ni$_4$(**pop**-H)$_4$(HCOOH)] + H}$^+$; 1198.96 (35), {[Ni$_4$(**pop**-H)$_4$(HCOOH)$_2$] + H}$^+$; 1244.95 (25), {[Ni$_4$(**pop**-H)$_4$(HCOOH)$_3$] + H}$^+$. IR (KBr) ν (cm^{-1}): 1525 (C=O$_{amid\ 1}$), 1080 (N–O$_{oxim}$).

[Cu$_4$(pop-H)$_4$(HCOOH)$_4$] (2). To a warm solution of H**pop** (0.022 g, 0.0001 mol) in 7/3 (v/v) methanol/DMSO (10 mL) was added a solution of Cu(CH$_3$COO)$_2$·H$_2$O (0.02 g, 0.0001 mol) and HCOOK (0.0084 g, 0.0001 mol) in water (10 mL) followed by 2 mL of 0.1 M KOH. The resulting mixture was stirred for 30 min and left for crystallization in air. After 40 days, green crystals were formed. The crystals were filtered off and washed with methanol. Yield: 47%.

ESI-MS, m/z (%): 846.5 (85), {[Cu$_3$(**pop**-H)$_3$] + H}$^+$; 883.4 (100), {[Cu$_3$(**pop**-H)$_3$] + K}$^+$; 1127.2 (100), {[Cu$_4$(**pop**-H)$_4$] + H}$^+$. IR (KBr) ν (cm^{-1}): 1635 (C=O$_{amid\ 1}$), 1087 (N–O$_{oxim}$).

[Cu$_4$(pop-H)$_4$(H$_2$O)$_4$]·9H$_2$O (3). To a solution of H**pop** (0.022 g, 0.0001 mol) in 1/1 (v/v) methanol/water (20 mL) was added Cu(CH$_3$COO)$_2$·H$_2$O (0.02 g, 0.0001 mol) followed by 2 mL of 0.1 M KOH. The resulting dark-green mixture was stirred with heating for 30 min and left for crystallization in air. Dark-green crystals were formed after 2 days. The crystals were filtered off and washed with methanol. Yield: 80%.

ESI-MS, m/z (%): 563.0 (45), {[Cu$_2$(**pop**-H)$_2$] + H}$^+$; 626.8 (60), {[Cu$_3$(**pop**-H)$_2$]}$^+$; 846.0 (30), {[Cu$_3$(**pop**-H)$_3$] + H}$^+$; 1127.1 (100), {[Cu$_4$(**pop**-H)$_4$] + H}$^+$. IR (KBr) ν (cm^{-1}): 1645 (C=O$_{amid\ 1}$), 1090 (N–O$_{oxim}$).

X-ray Crystallography. All of the measurements were performed using a Nonius KappaCCD diffractometer with a horizontally mounted graphite crystal as a monochromator and Mo Kα radiation. Data were collected and processed using Collect software.[25] The structures were solved and refined using the programs SHELXS-97 and SHELXL-97, respectively.[26] For structure representation, the program ORTEP-3 for Windows was used.[27]

For **1**, seven water molecules of crystallization were placed in the structure. One of the water molecules (O25) was disordered over two sites with occupancies of 0.6 and 0.4. Two other water molecules were refined with occupancies of 0.5. Because of the disorder, H atoms of water molecules were omitted. The NOH H atoms were placed on idealized positions using the CALCOH program.[28] Other H atoms were positioned geometrically and also were constrained to ride on their parent atoms, with C–H distances of 0.95–0.98 Å and U_{iso} = 1.2–1.5U_{eq}(parent atom). One of the HCOO$^-$ ligands was also disordered over two sites with occupancies of 0.61 and 0.39.

For **2**, the H atoms were positioned geometrically except for water hydrogen H5O, which was located using the difference Fourier map. The position of OH hydrogen H4O was determined using the CALCOH program. All of the H atoms were constrained to ride on their parent atoms, with U_{iso} = 1.2–1.5U_{eq}(parent atom).

For **3**, the H$_2$O hydrogen atoms were located using the difference Fourier map but constrained to ride on their parent atoms, with U_{iso} = 1.5U_{eq}(parent atom). Other H atoms were positioned geometrically and also were constrained to ride on their parent atoms, with C–H distances of 0.95–0.98 Å and U_{iso} = 1.2–1.5U_{eq}(parent atom). The highest peak was located 0.46 Å from atom O12. Five H$_2$O molecules were included in the asymmetric unit in the final refinement. No acceptable disorder model could be found for the residual electron density due to the additional solvent of crystallization. This electron density was handled using the SQUEEZE routine of PLATON,[29] leaving a void of 46 Å^3 in the structure.

Selected crystal data and refinement parameters for **1**–**3** are given in Table 1.

(25) *COLLECT*; Bruker AXS BV: Delft, The Netherlands, 2004.
(26) (a) Sheldrick, G. M. *SHELXS97*; University of Göttingen: Göttingen, Germany, 1997. (b) Sheldrick, G. M. *SHELXL97*; University of Göttingen: Göttingen, Germany, 1997.
(27) Farrugia, L. J. *J. Appl. Crystallogr.* **1997**, *30*, 565.
(28) Nardelli, M. *J. Appl. Crystallogr.* **1999**, *32*, 563–571.
(29) Spek, A. L. *J. Appl. Crystallogr.* **2003**, *36*, 7–13.

Table 2. Potentiometric and Spectroscopic Data for Proton and M^{2+} Complexes of **Hpop** (=HL) at 25 °C, with $I = 0.1$ M (KNO$_3$) and [**Hpop**] = 3 × 10^{-3} M

species	log β	log K	UV−vis		EPR	
			λ (nm)	ϵ (M^{-1} cm^{-1})	$A_{\parallel}$ (G)	$g_{\parallel}$
protonation of L						
HL	9.64(1)	9.64				
H$_2$L	13.30(2)	3.66				
Ni^{2+} complexes						
NiH$_2$L$_2$	26.39(3)		896	20		
NiHL$_2$	23.36(1)	3.03	890	27		
NiL$_2$	18.25(3)	5.11	881	52		
NiH$_{-2}$L$_2$	−3.25(4)		minor			
Ni$_2$H$_{-1}$L$_2$	20.43(4)		891	32		
Ni$_2$H$_{-2}$L$_2$	12.53(9)	7.9	minor			
Cu^{2+} complexes (Cu/L = 1/1)						
Cu$_3$H$_2$L$_3$	44.37(4)		659	72	not observed	
Cu$_3$HL$_3$	40.91(3)	3.46	656	81		
Cu$_3$L$_3$	35.99(3)	4.92	648	102		
Cu$_3$H$_{-1}$L$_3$	29.86(3)	6.13	645	120		
Cu$_3$H$_{-2}$L$_3$	22.61(4)	7.25	651	134		
Cu$_3$H$_{-3}$L$_3$	11.75(4)	10.86	651	134		
Cu^{2+} complexes (Cu/L = 1/2)						
CuHL$_2$	24.92(3)		663	21	147	2.30
CuL$_2$	20.99(3)	3.93	646	25	152	2.25
CuH$_{-1}$L$_2$	15.88(3)	5.11	642	29	179	2.19
CuH$_{-2}$L$_2$	9.16(3)	6.72	634	49	197	2.14

Results and Discussion

Synthesis. The ligand **Hpop** was obtained by reaction of 2-acetylpyridine with 2-(hydroxyimino)propanohydrazide in an ethanol/water solution at 60 °C and was fully characterized. The syntheses of complexes **1** and **2** were achieved via reaction of **Hpop** with Ni(NO$_3$)$_2$ and Cu(CH$_3$COO)$_2$ in water/methanol and water/methanol/DMSO solutions, respectively, in the presence of base (KOH) and formate anions. The formate anions were used as a structure-directing factor. On the other hand, reaction of **Hpop**, Cu(CH$_3$COO)$_2$, and KOH in a water/methanol solution without HCOO$^-$ gave compound **3**.

Protonation Constants. In order to evaluate the competition between protons and metal ions, it was first necessary to determine the acid−base properties of the studied ligand. **Hpop** showed two protonation constants, the first (log K_1 = 9.64) corresponding to the oxime OH group and the second (log K_2 = 3.66) to the pyridine N atom (Table 2).

Complex Formation in Solution. Nickel(II) Complexes. Calculations based on the potentiometric data obtained for the Ni^{2+}−**Hpop** system suggested the formation of the monomeric species NiH$_2$L$_2$, NiHL$_2$, NiL$_2$, and NiH$_{-2}$L$_2$ as well as the two dimeric complexes Ni$_2$H$_{-1}$L$_2$ and Ni$_2$H$_{-2}$L$_2$, where L is equal to **pop** (Table 2 and Figure 1A). Unfortunately, because of the minor differences in the ligand-field bands, the spectral parameters obtained from UV−vis spectroscopy did not define the coordination mode. The only spectroscopic feature seen was a band at 900 nm (ϵ = 20−50 M^{-1} cm^{-1}) that was observed over the whole pH range (Table 2), suggesting octahedral coordination of the Ni^{2+} ions.[30]

Formation of bis complexes starts from the NiH$_2$L$_2$ species, in which each ligand most likely acts as a bidentate {N$_2$}

ligand through its pyridine and hydrazone N atoms. Successive deprotonation of this complex (pK = 3.03 and 5.22) leads to the formation of NiHL$_2$ and NiL$_2$, respectively, in which the hydrazide O atoms become involved in metal coordination. The formation and identities of such 1/2 metal-to-ligand complexes were indeed confirmed by X-ray data for the mononuclear complex [Ni(**pop**-H)$_2$], which showed a six-coordinate metal ion with the ligands acting as tridentate {N$_2$O} donors (see Figure S1 in the Supporting Information).[31] The two subsequent deprotonations, which together produce NiH$_{-2}$L$_2$, may be assigned to the two noncoordinated oxime hydroxyl groups (Scheme 2A−C). Although only monomeric and dimeric Ni^{2+} species could be calculated on the basis of potentiometric data, the presence of species of higher nuclearity in solution was evidenced by ESI-MS and in the solid state by X-ray crystallographic analysis (described below).

Copper(II) Complexes. According to the potentiometric titrations performed for equimolar solutions of Cu^{2+} and **Hpop**, only trimeric species were found, starting with Cu$_3$H$_2$L$_3$ and ending with Cu$_3$H$_{-3}$L$_3$ (Table 2 and Figure 1B). The occurrence of the trimeric complexes was confirmed by ESI-MS. Also, the EPR spectra recorded for equimolar solutions of Cu^{2+} and **pop** provided evidence for the formation of oligomeric complexes, but this technique did not allow us to unambiguously distinguish whether these were dimeric or trimeric species. The spectra collected over the whole pH range studied (e.g., at pH 3, 4.5, 6, and 8) were flattened in comparison with those observed for 1/2 Cu^{2+}/**Hpop** solutions (Table 2 and Figure S2 in the Supporting Information). Coordination of Cu^{2+} started at the

(30) Meyer, F.; Kozłowski, H. In *Comprehensive Coordination Chemistry II*; McCleverty, J. A., Meyer, T. J., Eds.; Elsevier: Oxford, U.K., 2004; Vol. 6, pp 247−554.

(31) Moroz, Y. S.; Fritsky, I. O. *Visn. Kiiv. Nats. Univ. im. T. Shevchenka, Ser. Khim.* **2006**, *43*, 37−39. These data have been deposited with the Cambridge Crystallographic Data Centre (CCDC 675001) and can be obtained free of charge from the CCDC via www.ccdc.cam.ac.uk/data_request/cif.
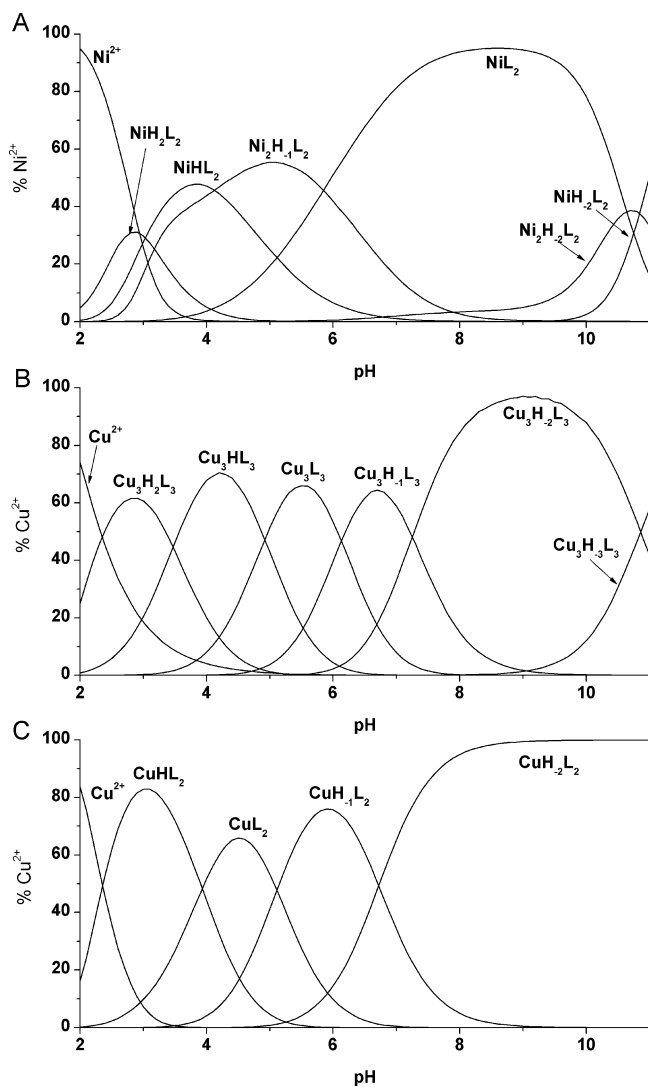
Figure 1. Species distribution profiles at 25 °C for (A) Ni^{2+} complexes of H**pop**, (B) Cu^{2+} complexes of H**pop** having a metal-to-ligand ratio of 1/1, and (C) Cu^{2+} complexes of H**pop** having a metal-to-ligand ratio of 1/2. In all cases, $I = 0.1$ M (using KNO_3) and [H**pop**] = 3×10^{-3} M.

Scheme 2. Possible Structures of the Species Formed in Solution
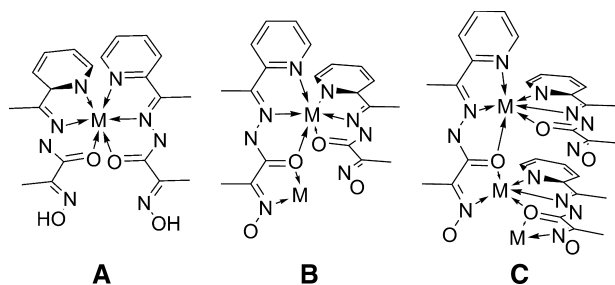
beginning of the pH range over which potentiometric studies were performed. Using UV−vis spectroscopy, we observed d−d transitions centered at 650 nm that appeared at pH 1.5 and showed little variation until the end of the pH range studied. While the exact constitution of the trimeric species is unknown, their structures are believed to resemble the one observed for the tetrameric species in the X-ray analysis except for the lack of one of the edges. Every Cu^{2+} ion is coordinated by two or three nitrogen donors: one from the pyridine ring, another from the hydrazone group, and
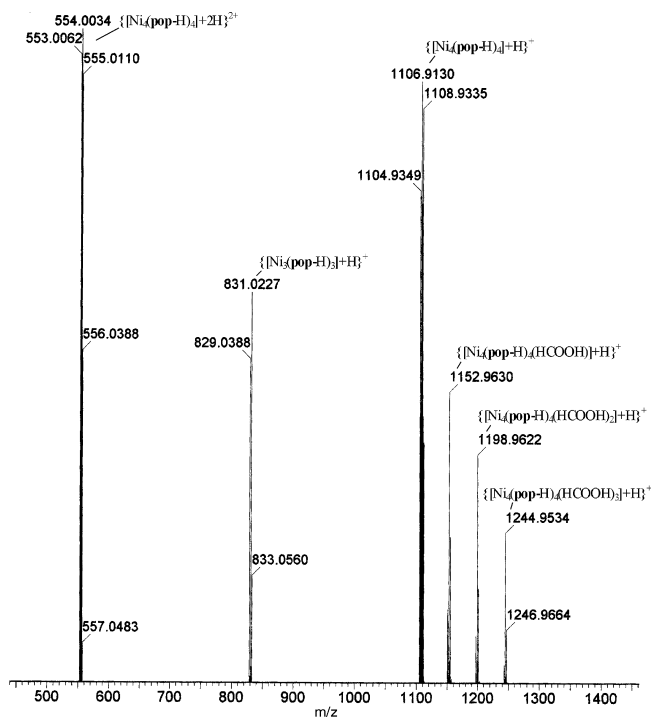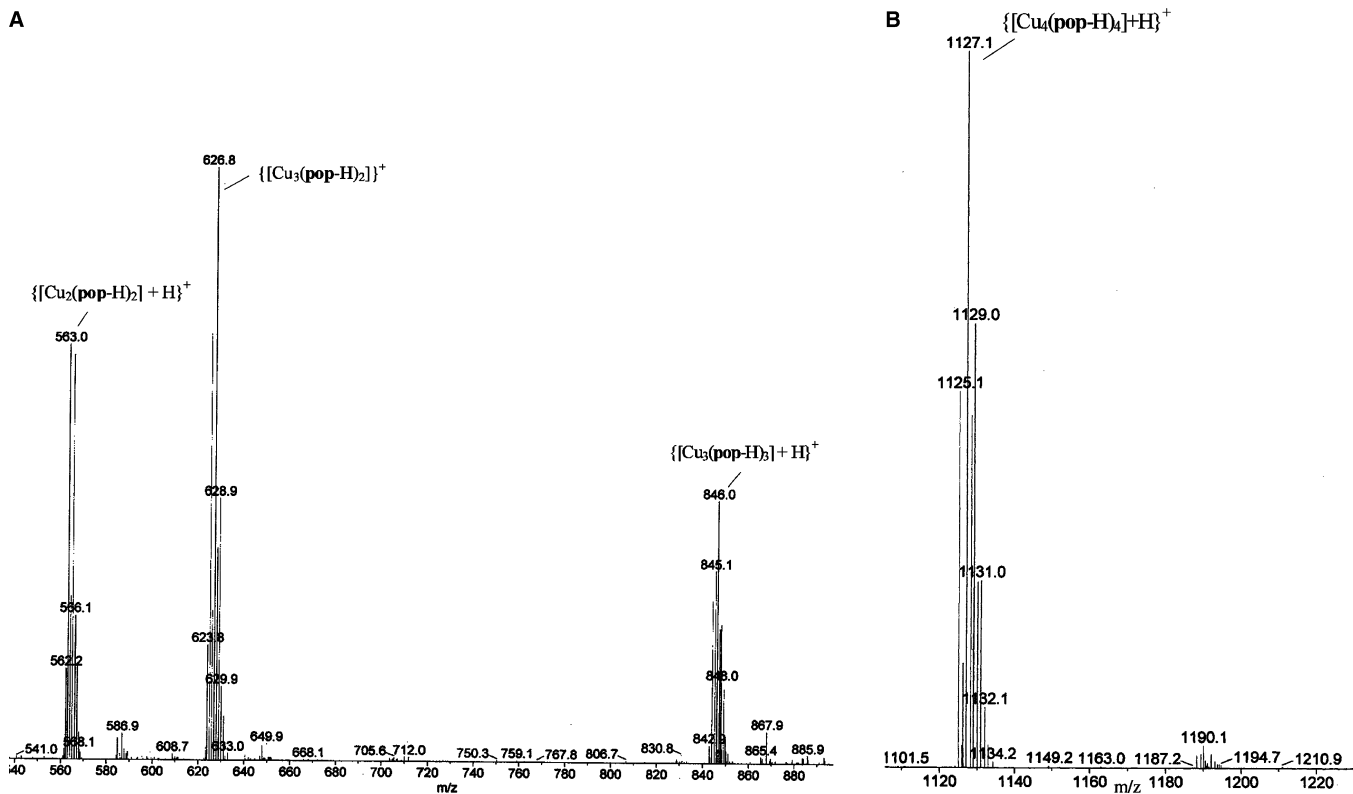
Figure 2. Fragment of the ESI-MS spectrum of the $Ni(NO_3)_2-$ H**pop**−HCOOH−KOH system (pH 9−10) in ethanol/water solution.

possibly a third from the N atom of the oxime group. The coordination sphere is completed by two oxygen atoms from hydrazone groups, which bridge two copper ions. The hydrolysis of $Cu_3H_{-2}L_3$ (log $K = 10.86$) suggests deprotonation of a water molecule.

Potentiometric titrations of the $Cu^{2+}-$H**pop** system for metal-to-ligand molar ratios of 1/2 and 1/3 allowed the identification of the four bis complexes $CuHL_2$ to $CuH_{-2}L_2$, where the coordination mode is most likely similar to that found for the $Ni^{2+}-$H**pop** complexes.

ESI Mass Spectrometry. Complex formation and the compositions of species in solution were monitored using ESI-MS. In the ESI-MS spectra of the synthesized Ni^{2+} and Cu^{2+} complexes, the presence of oligonuclear species was found to correlate in some cases with species identified by pH potentiometric titrations. In all cases, the main feature of the ESI-MS spectra was the presence of tetranuclear species, indicating that H**pop** exhibits a strong tendency to form oligonuclear complexes. Unfortunately, the nuclearity could not be deduced from calculations based on the pH potentiometric data because of similar expressions for the 1/1 and 4/4 metal/ligand species.

In the ESI-MS spectra of the $Ni(NO_3)_2-$H**pop**−HCOOH− KOH system (pH 9−10) in ethanol/water solution (Figure 2), peaks for six types of complex species were detected and attributed as follows: {[Ni_3(**pop**-H)_3] + H}$^+$ (m/z 831.02), {[Ni_4(**pop**-H)_4] + H}$^+$ (m/z 1106.91), {[Ni_4(**pop**-H)_4] + 2H}$^{2+}$ (m/z 554.00), {[Ni_4(**pop**-H)_4(HCOOH)] + H}$^+$ (m/z 1152.96), {[Ni_4(**pop**-H)_4(HCOOH)_2] + H}$^+$ (m/z 1198.96), and {[Ni_4(**pop**-H)_4(HCOOH)_3] + H}$^+$ (m/z 1244.95). The last three species are indicative of a stepwise dissociation path for the loss of formic acid from [Ni_4(**pop**-H)_4(HCOOH)_4]. The intensities of

A

B

Figure 3. Fragments of the ESI-MS spectra of CuX_2–H**pop**–HCOOH–KOH (pH 9–10) in DMSO/H_2O and CuX_2–H**pop**–KOH (pH 9–10) in methanol ($X = NO_3^-$, CH_3COO^-): (A) m/z 540–900; (B) m/z 1105–1230.

the signals were different, and the predominant species was $\{[Ni_4(\textbf{pop}\text{-H})_4] + 2H\}^{2+}$.

For the systems CuX_2–H**pop**–HCOOH–KOH (pH 9–10) in DMSO/H_2O and CuX_2–H**pop**–KOH (pH 9–10) in methanol ($X = NO_3^-$, CH_3COO^-), the spectra were very similar (Figure 3). On the other hand, for the CuX_2–H**pop**–HCOOH–KOH system (pH 9–10) in DMSO/H_2O, the stepwise dissociation of formic acid was not observed. The detected signals were ascribed as follows: $\{[Cu_2(\textbf{pop}\text{-H})_2] + H\}^+$ (m/z 563.0), $\{[Cu_3(\textbf{pop}\text{-H})_2]\}^+$ (m/z 626.8), $\{[Cu_3(\textbf{pop}\text{-H})_3] + H\}^+$ (m/z 846.0), and $\{[Cu_4(\textbf{pop}\text{-H})_4] + H\}^+$ (m/z 1127.1). The predominant species was $\{[Cu_4(\textbf{pop}\text{-H})_4] + H\}^+$ for both systems.

**Structural Studies. Molecular Structure of [Ni₄(pop)₄-(HCOO)₄]·7H₂O (1).** The molecular structure of **1** is illustrated in Figure 4A (with H atoms omitted for clarity); selected bond distances and angles are presented in Table 3. The compound consists of neutral $[Ni_4(\textbf{pop})_4(HCOO)_4]$ molecules and interstitial water molecules. The molecule $[Ni_4(\textbf{pop})_4(HCOO)_4]$ has a so-called [2 × 2] grid structure and consists of a rectangular cluster of four six-coordinate nickel(II) centers having the two pairs of parallel ligand strands arranged in a head-to-head fashion. The central ions are bridged by the amide oxygen atoms. Two of those oxygen atoms [O(3) and O(7)] are located above the mean Ni_4 plane, and two [O(1) and O(5)] are located below it; this results in a boatlike arrangement (Figure 4B). The grid has two different types of distorted square-bipyramidal chromophores, NiN_2O_4 and NiN_4O_2, with identical chromophores located at opposite corners of the grid.

NiN_2O_4 chromophores are formed by two nitrogen atoms belonging to the oxime groups, two oxygen atoms from the amide groups, and two oxygen atoms from the formate anions. The NiN_4O_2 chromophores include two oxygen atoms from the amide groups, two nitrogen atoms belonging to the azomethine groups, and two nitrogen atoms from the pyridine rings. The Ni–O and Ni–N bond lengths and N–Ni–N′, O–Ni–N, and O–Ni–O′ bond angles (Table 3) are typical of previously reported octahedral Ni^{2+} complexes with amide- and pyridine-containing ligands.[30,32] Each ligand forms three five-membered chelate rings. An additional seven-membered pseudochelate ring at the NiN_2O_4 chromophore is produced by formation of an intramolecular hydrogen bond in which the donor is the oxime group and the acceptor is the formate anion. According to the X-ray data, the amide groups are deprotonated and O-coordinated (Table 3).

The Ni···Ni′ separations in the grid are close to 4 Å [Ni(1)–Ni(2), 3.920(1) Å; Ni(1)–Ni(4), 3.955(1) Å; Ni(2)–Ni(3), 3.962(1) Å; Ni(3)–Ni(4), 3.898(1) Å], and the Ni–O–Ni′ angles fall in the range 137.6–138.6° [Ni(1)–O(1)–Ni(4), 138.1(2)°; Ni(2)–O(3)–Ni(1), 137.6(2)°; Ni(2)–O(5)–Ni(3), 138.54(15)°; Ni(4)–O(7)–Ni(3), 137.7(2)°]. In the unit cell, the tetranuclear molecules are connected by a complex system of hydrogen bonds.

Molecular Structures of [Cu₄(pop-H)₄(HCOOH)₄]·H₂O (2) and [Cu₄(pop-H)₄(H₂O)₄]·9H₂O (3). The molecular structure of **2** is illustrated in Figure 5A (with H atoms

(32) Świątek-Kozłowska, J.; Fritsky, I. O.; Dobosz, A.; Karaczyn, A.; Dudarenko, N. M.; Sliva, T. Y.; Gumienna-Kontecka, E.; Jerzykiewicz, L. *J. Chem. Soc., Dalton Trans.* **2000**, 4064–4068.
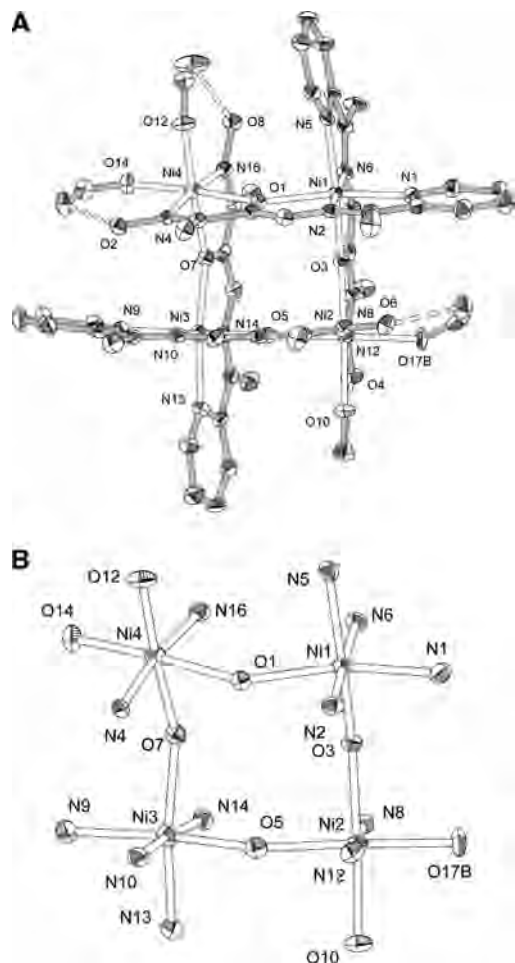
Figure 4. Structural representations of (A) compound **1** and (B) its tetranuclear nickel(II) cluster. Displacement ellipsoids are shown at the 30% probability level. Hydrogen bonds are indicated by dashed lines.

Figure 5. Structural representation of (A) compound **2** and (B) its tetranuclear copper(II) cluster. Displacement ellipsoids are shown at the 30% probability level. Hydrogen bonds are indicated by dashed lines.

omitted for clarity); selected bond distances and angles are presented in Table 4. The compound consists of neutral $[Cu_4(\text{pop-}H)_4(HCOOH)_4]$ molecules and interstitial water molecules. Similar to **1**, $[Cu_4(\text{pop-}H)_4(HCOOH)_4]$ also adopts a $[2 \times 2]$ grid structure and features a tetranuclear copper(II) cluster having six-coordinate metal ions at the corners. The metal ions are bridged by the amide oxygen atoms, forming a boatlike Cu_4O_4 arrangement similar to that in **1** (with two oxygens located above and two located below the mean Cu_4 plane) (Figure 5B). However, in contrast to **1**, the grid in **2** has S_4 point symmetry. This results from a head-to-tail arrangement of the ligand strands, leading to the formation of only one type of chromophore, CuN_3O_3, which consists of three nitrogen atoms (belonging to the azomethine group and the pyridine ring from one ligand and the oxime group from the other ligand) and three oxygen atoms (one from each of two different amide groups and the coordinated molecule of formic acid). The chromophore has a distorted square-bipyramidal arrangement. The Cu−O and Cu−N bond lengths and N−Cu−N′, O−Cu−N, and O−Cu−O′ bond angles (Table 4) are very similar to those previously reported for octahedral Cu^{2+} complexes with amide- and pyridine-containing ligands. Each ligand forms three five-membered chelate rings. An additional seven-membered

pseudochelate ring is formed by an intramolecular hydrogen bond that differs from the one in **1**; in the H bond of **2**, the donor is the molecule of formic acid, and the acceptor is the deprotonated oxime group of H**pop**. According to the X-ray data, the amide groups are again deprotonated and O-coordinated (Table 4).

The Cu···Cu′ separations are close to 4 Å [Cu(1)−Cu(1)′, 4.120(6) Å], and the Cu−O−Cu′ angles are 142.2(1)°. In the crystal, the elements of the structure are connected by hydrogen bonds in which solvated water molecules act as donors and coordinated HCOOH molecules as acceptors.

The molecular structure of **3** is illustrated in Figure 6A (with H atoms omitted for clarity); selected bond distances and angles are collected in Table 5. The compound consists of neutral $[Cu_4(\text{pop-}H)_4(H_2O)_4]$ molecules and interstitial water molecules.

The molecular structure of $[Cu_4(\text{pop-}H)_4(H_2O)_4]$ is basically identical to that of **2**. It forms a tetranuclear rectangular $[2 \times 2]$ gridlike aggregate consisting of six-coordinate copper(II) ions and two mutually perpendicular pairs of **pop**-H ligand strands. The molecule has a (noncrystallographic) S_4 symmetry axis that passes through the center of the Cu_4 square. Each copper(II) ion has a CuN_3O_3 donor arrangement. The three nitrogen atoms come from the

Table 3. Selected Bond Distances (Å) and Angles (deg) for **1**

Ni(1)−N(2)	1.973(6)	Ni(4)−N(4)	2.059(6)	N(6)−Ni(1)−N(5)	78.6(2)
Ni(1)−N(6)	1.988(6)	Ni(4)−O(7)	2.069(5)	N(10)−Ni(3)−N(13)	98.7(3)
Ni(1)−N(5)	2.072(6)	Ni(4)−O(14)	2.087(5)	N(14)−Ni(3)−N(13)	78.8(3)
Ni(1)−N(1)	2.116(6)	Ni(4)−O(1)	2.118(5)	N(10)−Ni(3)−N(9)	77.9(3)
Ni(1)−O(1)	2.117(5)	N(2)−Ni(1)−N(1)	77.8(3)	N(14)−Ni(3)−N(9)	105.7(3)
Ni(1)−O(3)	2.122(5)	N(6)−Ni(1)−N(1)	99.5(3)	N(13)−Ni(3)−N(9)	92.8(3)
Ni(1)···Ni(2)	3.920(1)	N(5)−Ni(1)−N(1)	96.6(2)	N(10)−Ni(3)−O(7)	106.3(2)
Ni(1)···Ni(4)	3.955(1)	N(2)−Ni(1)−O(1)	76.9(2)	N(14)−Ni(3)−O(7)	76.3(2)
Ni(2)−N(12)	2.009(6)	N(6)−Ni(1)−O(1)	105.9(2)	N(9)−Ni(3)−O(7)	91.7(2)
Ni(2)−N(8)	2.035(6)	N(5)−Ni(1)−O(1)	88.6(2)	N(10)−Ni(3)−O(5)	76.8(2)
Ni(2)−O(16A)	2.04(2)	N(6)−Ni(1)−O(3)	76.4(2)	N(14)−Ni(3)−O(5)	99.69(19)
Ni(2)−O(10)	2.069(5)	N(1)−Ni(1)−O(3)	93.6(2)	N(13)−Ni(3)−O(5)	92.5(2)
Ni(2)−O(3)	2.083(5)	O(1)−Ni(1)−O(3)	92.28(18)	O(7)−Ni(3)−O(5)	93.97(16)
Ni(2)−O(5)	2.112(3)	N(12)−Ni(2)−O(16A)	82.2(4)	O(12)−Ni(4)−N(16)	101.0(2)
Ni(2)−O(17B)	2.12(4)	N(8)−Ni(2)−O(16A)	96.5(4)	O(12)−Ni(4)−N(4)	83.7(2)
Ni(2)···Ni(3)	3.962(1)	N(12)−Ni(2)−O(10)	84.1(2)	N(16)−Ni(4)−O(7)	78.4(2)
Ni(3)−N(10)	1.986(6)	N(8)−Ni(2)−O(10)	102.2(2)	N(4)−Ni(4)−O(7)	96.6(2)
Ni(3)−N(14)	1.991(6)	O(16A)−Ni(2)−O(10)	91.3(5)	O(12)−Ni(4)−O(14)	94.2(2)
Ni(3)−N(13)	2.086(6)	N(12)−Ni(2)−O(3)	96.2(2)	N(16)−Ni(4)−O(14)	82.2(2)
Ni(3)−N(9)	2.095(7)	N(8)−Ni(2)−O(3)	77.6(2)	N(4)−Ni(4)−O(14)	102.9(2)
Ni(3)−O(7)	2.110(5)	O(16A)−Ni(2)−O(3)	90.7(4)	O(7)−Ni(4)−O(14)	89.3(2)
Ni(3)−O(5)	2.124(3)	N(12)−Ni(2)−O(5)	77.0(2)	O(12)−Ni(4)−O(1)	89.6(2)
Ni(3)···Ni(4)	3.898(1)	O(10)−Ni(2)−O(5)	88.32(18)	N(16)−Ni(4)−O(1)	97.8(2)
Ni(4)−O(12)	2.039(5)	O(3)−Ni(2)−O(5)	89.76(15)	N(4)−Ni(4)−O(1)	76.8(2)
Ni(4)−N(16)	2.047(6)	N(2)−Ni(1)−N(5)	98.6(2)	O(7)−Ni(4)−O(1)	86.98(18)

**Table 4.** Selected Bond Distances (Å) and Angles (deg) for **2**[a]

Cu(1)−N(2)	1.935(3)	Cu(1)−N(4)	2.001(3)
Cu(1)−O(1)	2.030(2)	Cu(1)−N(1)	2.057(3)
Cu(1)−O(1)′	2.323(2)	Cu(1)−O(3)	2.324(2)
Cu(1)···Cu(1)′	4.1195(6)	O(1)−C(8)	1.291(4)
N(4)−Cu(1)−O(1)	101.15(10)	N(2)−Cu(1)−O(1)	78.51(10)
N(4)−Cu(1)−N(1)	100.33(11)	N(2)−Cu(1)−N(1)	79.69(11)
N(2)−Cu(1)−O(1)′	101.37(9)	N(4)−Cu(1)−O(1)′	74.96(9)
O(1)−Cu(1)−O(1)′	90.26(11)	N(1)−Cu(1)−O(1)′	89.99(9)
N(2)−Cu(1)−O(3)	85.67(10)	N(4)−Cu(1)−O(3)	97.96(10)
O(1)−Cu(1)−O(3)	85.36(9)	N(1)−Cu(1)−O(3)	97.11(10)

[a] Symmetry transformation used to generate equivalent atoms: y, $-x + \frac{1}{2}$, $-z + \frac{1}{2}$.

pyridine, azomethine, and oxime groups; two of the three oxygen atoms belong to the amide groups, and one belongs to a water molecule. Compared with **2**, the formic acid ligands have been replaced by water. The CuN_3O_3 chromophore in **3** has a severely distorted square-bipyramidal arrangement (4 + 1 + 1). The Cu−O and Cu−N bond distances and N−Cu−N′, O−Cu−N, and O−Cu−O′ bond angles (Table 5) are typical for square-bipyramidal Cu(II) with pronounced Jahn−Teller distortion. The **pop**-H ligands form three five-membered chelate rings (Figure 6B).

The metal ions in **3** are bridged by the amide oxygen atoms; the Cu···Cu′ separations are close to 4 Å [3.9864(6) Å], and the Cu−O−Cu′ angles are 139.25(13)° [Cu(2)−O(3)−Cu(1)] and 140.00(13)° [Cu(1)−O(1)−Cu(2)′]. The oxime N−O and C−N and amide C−N and C−O bond distances suggest that these groups are deprotonated (Table 5). In the crystal lattice, the elements of the structure are connected by single and bifurcated H bonds.

Structural Isomerism. After deprotonation, H**pop** provides two different potential chelating compartments. One of these (the "head") contains three donor functions, namely, the pyridine, azomethine, and amide groups; the other one (the "tail") contains two donor functions, namely, the amide and oxime groups. Such a ligand topology can give rise to the formation of isomeric grids (head-to-head, head-to-tail, etc.). We suggest that the main reason favoring formation
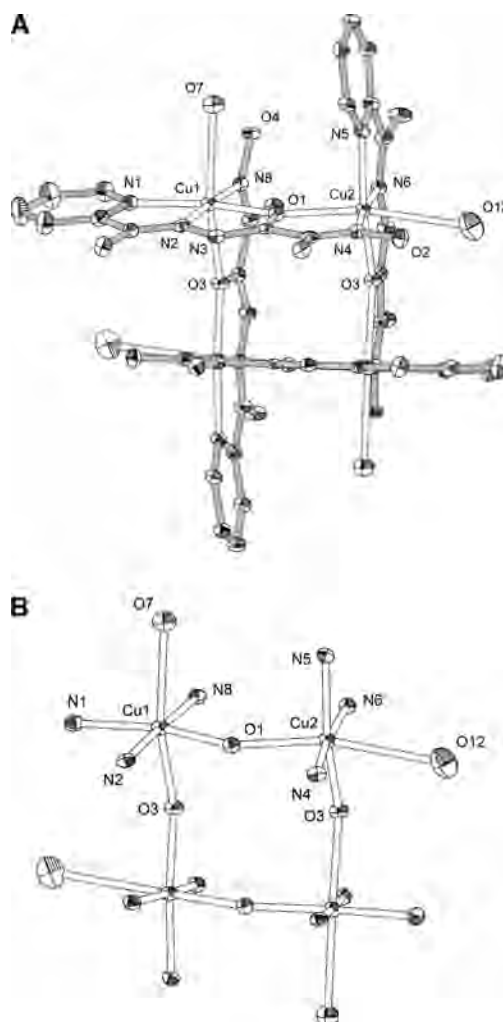

Figure 6. Structural representation of (A) compound **3** and (B) its tetranuclear copper(II) cluster. Displacement ellipsoids are shown at the 30% probability level.

of a particular isomer is the nature of the central ion. This factor probably governs the different ways that grids self-

**Table 5.** Selected Bond Distances (Å) and Angles (deg) for 3^a

Cu(1)−N(2)	1.937(3)	N(2)−Cu(1)−O(1)	78.57(13)
Cu(1)−N(8)	1.985(3)	N(8)−Cu(1)−O(1)	99.70(12)
Cu(1)−O(1)	2.002(3)	N(2)−Cu(1)−N(1)	79.79(14)
Cu(1)−N(1)	2.039(4)	N(8)−Cu(1)−N(1)	101.92(14)
Cu(1)−O(3)	2.276(3)	N(2)−Cu(1)−O(3)	102.42(11)
Cu(1)−O(7)	2.539(3)	N(8)−Cu(1)−O(3)	75.85(11)
Cu(1)···Cu(2)	3.9864(6)	O(1)−Cu(1)−O(3)	92.05(10)
Cu(2)−N(6)	1.930(3)	N(1)−Cu(1)−O(3)	92.31(12)
Cu(2)−N(4)	1.954(3)	N(2)−Cu(1)−O(7)	98.92(11)
Cu(2)−O(3)	1.975(2)	N(8)−Cu(1)−O(7)	82.77(11)
Cu(2)−N(5)	2.013(3)	O(1)−Cu(1)−O(7)	90.56(10)
Cu(2)−O(1)′	2.202(3)	N(1)−Cu(1)−O(7)	93.04(12)
Cu(2)−O(12)	2.830(9)	N(6)−Cu(2)−O(3)	79.31(12)
N(2)−Cu(1)−N(8)	177.56(13)	N(4)−Cu(2)−O(3)	100.84(12)
O(3)−Cu(2)−O(1)′	97.70(11)	N(6)−Cu(2)−N(5)	80.64(13)
N(5)−Cu(2)−O(1)′	90.94(11)	N(4)−Cu(2)−N(5)	98.76(13)
N(6)−Cu(2)−O(12)	94.53(18)	O(3)−Cu(2)−N(5)	159.81(12)
N(4)−Cu(2)−O(12)	78.60(18)	N(6)−Cu(2)−O(1)′	108.72(12)
O(3)−Cu(2)−O(12)	81.9(2)	N(4)−Cu(2)−O(1)′	78.23(12)
N(5)−Cu(2)−O(12)	97.3(2)		

^{a} Symmetry transformation used to generate equivalent atoms: $-x + \frac{1}{2}, y, -z + \frac{1}{2}$.

Scheme 3. Proposed Scheme for the Formation of Nickel-Containing Grids
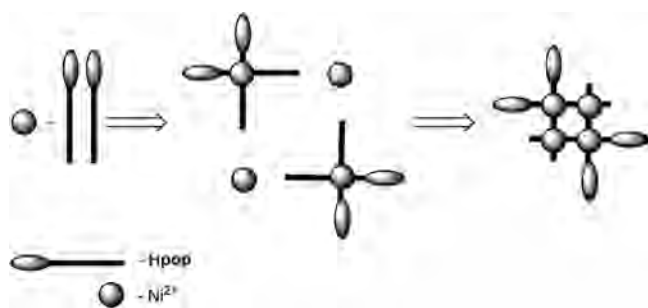
assemble. The formation of the nickel-containing grid is likely to proceed via a two-step self-assembly process (Scheme 3). It is known that for high-spin Ni^{2+} complexes, realization of octahedral coordination is favored, and in the first step, an [Ni(**pop**)$_2$] species in which the ligands are disposed head-to-head is formed. The corresponding complex was obtained and characterized by IR spectroscopy, ESI-MS, and single-crystal X-ray analysis.[31] In the second step, two such [Ni(**pop**)$_2$] species are aggregated with two additional Ni^{2+} ions to give the grid. For the copper grids, one-step self-assembly seems to be more likely. The [Cu$_4$(**pop**-H)$_4$] species were detected in solution by ESI-MS, and for Cu^{2+} ions, the head-to-tail arrangement of the ligands appears to be preferred. In this case, only five coordination sites of the central ion are occupied, in agreement with the tendency of a copper(II) ion to decrease its coordination number because of Jahn−Teller distortion. The sixth coordination site can thus be vacant or occupied by a distant monodentate ligand (water or formate), as seen from the X-ray results.

Magnetic Properties. Variable-temperature magnetic susceptibility data for compounds **1** and **3** were obtained in the temperature range 1.8−300 K, and measurements of magnetization as a function of field were performed. The magnetic moment of **1** at room temperature was 2.95 μ_B per metal ion, which is typical for high-spin Ni^{2+} and slightly greater than the expected spin-only value. Compound **3** had a room-temperature moment of 1.80 μ_B per metal ion, which
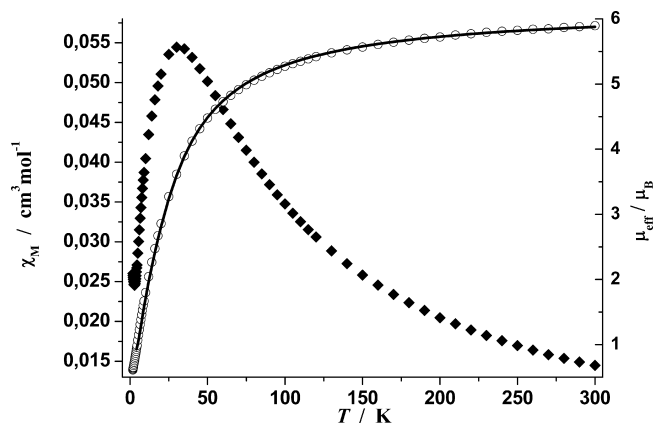
Figure 7. Plots of χ_M (◆) and μ_{eff} (○) as functions of T for **1**. The solid line represents the simulated curve.

is a typical value for copper(II).

The susceptibility (χ_M) of **1** showed a sharp maximum at 30 K as the temperature was decreased (◆ in Figure 7), indicating the presence of intramolecular antiferromagnetic coupling. The plot of μ_{eff} (per mole) versus temperature (○ in Figure 7) shows that the value of μ initially decreased only slightly on cooling, from 5.88μ_B at 300 K to 5.14μ_B at 85 K, after which it decreased more rapidly, reaching 0.61μ_B at 1.8 K.

A simulation of these variable-temperature magnetic data was based on an isotropic exchange expression derived from the Hamiltonian (eq 1) for a square arrangement of four magnetically identical $S = 1$ metal centers:

$$\hat{H} = -2J(\hat{\mathbf{S}}_1 \cdot \hat{\mathbf{S}}_2 + \hat{\mathbf{S}}_2 \cdot \hat{\mathbf{S}}_3 + \hat{\mathbf{S}}_3 \cdot \hat{\mathbf{S}}_4 + \hat{\mathbf{S}}_4 \cdot \hat{\mathbf{S}}_1) \quad (1)$$

The total spin-state combinations and their energies were calculated using the Kambe approach,[33] and the data were fitted using the MAGMUN 4.1 software.[34]

The best fit calculated for **1** gave the following parameter values: $g = 2.186(3)$, $J = -14.7(1)$ cm^{-1}, $\rho = 0.02$, $\theta = -2.4$ K, and $R = 9.7 \times 10^{-3}$, where ρ is the fraction of paramagnetic impurity, θ is a Weiss-like temperature correction, $R = [\sum(X_{obs} - X_{calc})^2/\sum X_{calc}^2]^{1/2}$, and all of the other parameter symbols have their usual meaning. The presence of antiferromagnetic exchange coupling is entirely consistent with a structure in which the four nickel(II) ions are bridged by amide oxygen atoms with values for the Ni−O−Ni angles in the range 137.6−138.6°, in agreement with magnetostructural findings reported previously for related complexes.[16,17]

The variable-temperature magnetic data for the copper(II) grid **3** showed different behavior, namely, a steady increase in χ_M upon cooling, without maximum in this case (◆ in Figure 8). The plot of μ_{eff} (per mole) versus temperature (○ in Figure 8) shows that μ_{eff} first slightly decreased, from 3.6μ_B at 300 K to 3.56μ_B at 115 K, but then rose sharply to 4.42μ_B at 3.64 K. This is clearly indicative of ferromagnetic behavior. The slight decrease in μ_{eff} at very low temperatures (3.64−1.8 K) may indicate the presence of an intermolecular antiferromagnetic component or zero-field splitting. The data were fitted over the temperature range 4−300 K using a procedure similar to that for **1**, based on an isotropic

(33) Kambe, K. *J. Phys. Soc. Jpn.* **1950**, *5*, 48−51.
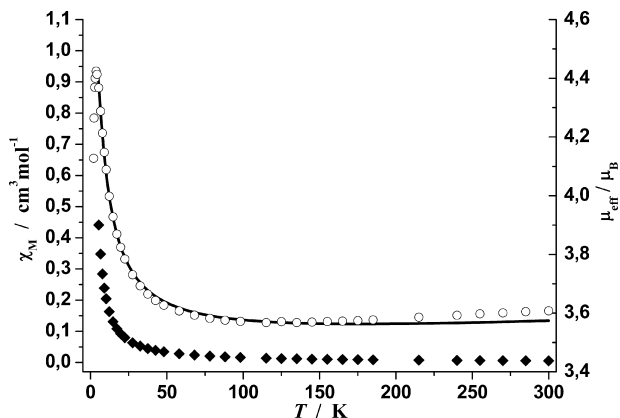
Figure 8. Plots of χ_M (◆) and μ_{eff} (○) as functions of T for **3**. The solid line represents the simulated curve.

exchange expression derived from the Hamiltonian (eq 1) for a square arrangement of four magnetically identical $S = {}^1/_2$ metal centers.

The parameter values obtained from the fit were $g = 2.011(3)$, $J = 6.2(2)$ cm^{-1}, $\rho = 0$, $P_{TI} = 200 \times 10^{-6}$ emu mol^{-1}, $\theta = -0.34$ K, and $R = 3.39 \times 10^{-3}$, where P_{TI} is the temperature-independent paramagnetism. The positive value of J confirms the presence of predominant intramolecular ferromagnetic coupling. A small negative value of θ can be associated with a weak intermolecular antiferromagnetic exchange interaction between the translational grids, as mentioned above. The predominant intramolecular ferromagnetic exchange in **3** may be explained in terms of a strictly orthogonal orientation of the d$_{x^2-y^2}$ magnetic orbitals of neighboring metal ions[35] and is in agreement with previously reported data for several copper-containing [2 × 2] grids.[12,16] The observation of fundamental differences in the magnetic behaviors of nickel(II) and copper(II) grids of the same ligand is in agreement with previous reports for grid complexes of this type.[16]

Conclusions

A new, easily prepared polynucleating oxime-containing ligand (**Hpop**) has been successfully used with copper(II) and nickel(II) salts to obtain a series of [2 × 2] molecular grids that arise from a selective self-assembly process. In all of the grid complexes, the metal ions are six-coordinate: five donor sites are occupied by **pop**-H, and the sixth is available for labile coligands (water or HCOO$^-$/HCOOH). As a special feature of the **pop**-H scaffolds, these grids have noncoordinated O atoms from the oxime groups, which usually are considered as good bridging groups.[36,37] These accessible O atoms at the periphery of the grid might be useful for further linking of the grid structures into higher-dimensional networks. Replacement of the labile coligands (water or HCOO$^-$/HCOOH) by potentially bridging ligands should be an alternative approach in this direction. Such studies are currently underway in our laboratories.

Supporting Information Available: X-ray crystallographic files (in CIF format) for the structure determinations of [Ni$_4$-(**pop**)$_4$(HCOO)$_4$]·7H$_2$O (**1**), [Cu$_4$(**pop**-H)$_4$(HCOOH)$_4$]·H$_2$O (**2**), and [Cu$_4$(**pop**-H)$_4$(H$_2$O)$_4$]·9H$_2$O (**3**); a structural representation of [Ni(**pop**)$_2$]·2H$_2$O; and EPR spectra of Cu^{2+}−H**pop** systems. This material is available free of charge via the Internet at http://pubs.acs.org.

IC702375H

(34) Xu, Z.; He, K.; Thompson, L. K.; Waldman, O. *MAGMUN 4.1*; Memorial University of Newfoundland: St. John's, NL, 2002.
(35) Kahn, O. *Molecular Magnetism*; VCH Publishers, Inc.: New York, 1993.
(36) Kanderal, O. M.; Kozłowski, H.; Dobosz, A.; Świątek-Kozłowska, J.; Meyer, F.; Fritsky, I. O. *Dalton Trans.* **2005**, 1428–1437.
(37) Fritsky, I. O.; Kozłowski, H.; Kanderal, O. M.; Haukka, M.; Świątek-Kozłowska, J.; Gumienna-Kontecka, J.; Meyer, F. *Chem. Commun.* **2006**, *39*, 4125–4127.